Factors affecting carbon-14 activity of unsaturated zone CO_2 and implications for groundwater dating

Cameron Wood [a,*], Peter G. Cook [a,b], Glenn A. Harrington [a,c], Karina Meredith [d], Rolf Kipfer [e]

[a] National Centre for Groundwater Research and Training, School of the Environment, Flinders University, South Australia, Australia
[b] CSIRO Water for a Healthy Country National Research Flagship, Adelaide, South Australia, Australia
[c] Innovative Groundwater Solutions, Blackwood, South Australia, Australia
[d] ANSTO, Institute for Environmental Research, New South Wales, Australia
[e] Swiss Federal Institute of Aquatic Science and Technology, Switzerland

ARTICLE INFO

SUMMARY

Unsaturated zone processes may influence the carbon-14 (^{14}C) activity of infiltrating groundwater and thus introduce error in derived groundwater residence times. However unsaturated zone ^{14}C activities are rarely measured and there is little understanding of how they may vary spatially in a groundwater basin. In this study we measured ^{14}C activity in unsaturated zone gas at five sites with different water-table depths (8.2–31.5 m) in the arid Ti Tree Basin, central Australia. We observed a relatively uniform decrease in ^{14}C activity of unsaturated zone gas with depth at most sites, with variation in unsaturated zone depths leading to variation in ^{14}C activities directly above the watertable at each site (ranging from 54 to 106 percent Modern Carbon (pMC)). Through modelling we show that the profiles are influenced by CO_2 production at different depths from sources with different isotopic ratios, including production of 'modern' CO_2 in the root zone and production of 'old' CO_2 above the watertable. Scenario modelling showed that these processes are independent of recharge when recharge is low (0–10 mm y^{-1}) but that higher recharge rates (>100 mm y^{-1}) result in more advective transport of atmospheric CO_2 to the water-table. The variation in ^{14}C above the watertable was more sensitive to watertable depth and shallow and deep CO_2 production rates. These findings offer insight into how unsaturated zone ^{14}C activities may vary spatially and provide guidance as to when ^{14}C depletion in unsaturated zone CO_2 may become important for groundwater dating, particularly in arid settings.

© 2014 Elsevier B.V. All rights reserved.

1. Introduction

Carbon-14 (^{14}C) has been widely used as a tracer in groundwater studies to investigate groundwater residence time, groundwater recharge and its spatial and temporal variability, and regional flow characteristics (Vogel, 1967; Love et al., 1993; Harrington et al., 2002). A consistent problem in interpreting ^{14}C activities in groundwater is accounting for reactions and processes other than radioactive decay that may alter the ^{14}C activity (such as dilution caused by carbonate weathering and oxidation of 'old' organic matter) and determining the ^{14}C activity at the time of recharge. Geochemical mass balance models are typically used to correct for carbonate weathering and assign an initial ^{14}C activity at the time of recharge (Ingerson and Pearson, 1964; Tamers, 1975; Fontes and Garnier, 1979). Accurate calculation of the initial ^{14}C activity also requires

knowledge of the ^{14}C activity of unsaturated zone gas, however this is rarely measured and typically assumed to be in equilibrium with atmospheric CO_2 (Mazor, 2004).

Several studies have shown that ^{14}C activities in unsaturated zone CO_2 can be depleted relative to atmospheric CO_2 (Haas et al., 1983; Leaney and Allison, 1986; Yang et al., 1994; Thorstenson et al., 1998; Keller and Bacon, 1998) and the implications for groundwater age calculation may be significant (Bacon and Keller, 1998). Keller and Bacon (1998) reported unsaturated zone ^{14}C activities of 20 pMC in a 7 m deep profile in Saskatchewan, Canada. This depletion of ^{14}C was caused by oxidation of old (low ^{14}C) organic matter near the watertable, and hence production of old CO_2. They presented a model of unsaturated zone ^{14}C transport (with diffusion in the gas phase being the dominant transport process) with two isotopically distinct zones of CO_2 production: a shallow zone of CO_2 production with an atmospheric ^{14}C activity (representing plant root respiration) and a deeper zone of CO_2 production with a depleted ^{14}C activity (from oxidation of organic

matter). Walvoord et al. (2005) reported unsaturated zone ^{14}C activity of 20 pMC in a 110 m deep profile in the Amargosa Desert, USA, and likewise replicated their profile with a gas transport model that considers shallow and deep zones of CO_2 production with different isotope signatures. However Walvoord et al. (2005) considered the source of deep older CO_2 to be calcite precipitation at a slowly declining watertable. Walvoord et al. (2005) also assessed the sensitivity of ^{14}C profiles to shallow 'modern' CO_2 production (in a 1 m thick root zone) and deep 'old' CO_2 production, however the influence of other processes such as recharge rate, root zone thickness and watertable depth was not assessed.

These studies demonstrate both the importance of measuring ^{14}C in the unsaturated zone and provide a conceptual understanding of the controlling processes. However despite the wealth of studies that have used ^{14}C activities to date groundwater, there remains a paucity of measured unsaturated zone ^{14}C profiles in the literature (approximately 7 profiles to the authors knowledge that are >10 m in depth (Thorstenson et al., 1983; Haas et al., 1983; Suchomel et al., 1990; Leaney and Allison, 1986; Striegl and Healy, 1990; Yang et al., 1996; Keller and Bacon, 1998; Walvoord et al., 2005). Most of the previous studies are limited to one to two profiles and are in arid settings, hence limiting their assessment of spatial variability in unsaturated zone ^{14}C, and how understanding of the controlling processes may be transferred to other locations. Consequently there is a poor understanding of when unsaturated zone processes are likely to alter the ^{14}C activity of unsaturated zone gas, and the difficulties in interpreting ^{14}C activities in groundwater persist (Herczeg and Leaney, 2011).

In this study we measured unsaturated zone ^{14}C activities at five sites with different watertable depths in the arid Ti Tree Basin, central Australia, providing insight into spatial variability in unsaturated zone ^{14}C activity. We interpret and model our data in terms of CO_2 production in the unsaturated zone from sources with different carbon isotope compositions, consistent with previous studies. Diffusive transport is constrained by measurements and modelling of chlorofluorocarbons (CFCs) in the unsaturated zone (rather than measuring porosity and assuming a value for tortuosity, which may be poorly constrained in gravelly sediments (Walvoord et al., 2005)). This enables CO_2 production rates to be much more accurately determined. We then evaluate the influence of recharge rate, and shallow and deep CO_2 production on unsaturated zone ^{14}C profiles over a range of watertable depths. This sensitivity analysis draws attention to the factors most likely to affect ^{14}C activity at the watertable, and demonstrates how spatial variability in ^{14}C activity at the watertable may arise. These findings help constrain the conditions under which dilution of the ^{14}C activity of unsaturated zone CO_2 may occur, and act as a guide as to when these unsaturated zone processes need to be considered in groundwater dating studies.

2. Study area

The Ti Tree Basin covers an area of ~5500 km^2 and is located 150 km north of Alice Springs in central Australia (Fig. 1). Mean annual rainfall is low (300 mm y^{-1}) and occurs mostly in the southern hemisphere summer (December–March). Soil types are generally either dark red massive clays that support predominantly Mulga vegetation (*Acacia* spp.) or red earthy sands that are dominated by Spinifex grass (*Trioda* spp.) under a sparse open woodland of bloodwood (*Corymbia* spp.) and coolabah trees (*Eucalyptus* spp.). The basin is comprised of Tertiary lacustrine and fluviatile sediments which make up the main unconfined aquifer (undifferentiated sandstone, limestone and silty sandstone). Depth to groundwater ranges from >60 m in the southern portion of the basin to <10 m in the north (Fig. 1). Observation wells in shallower
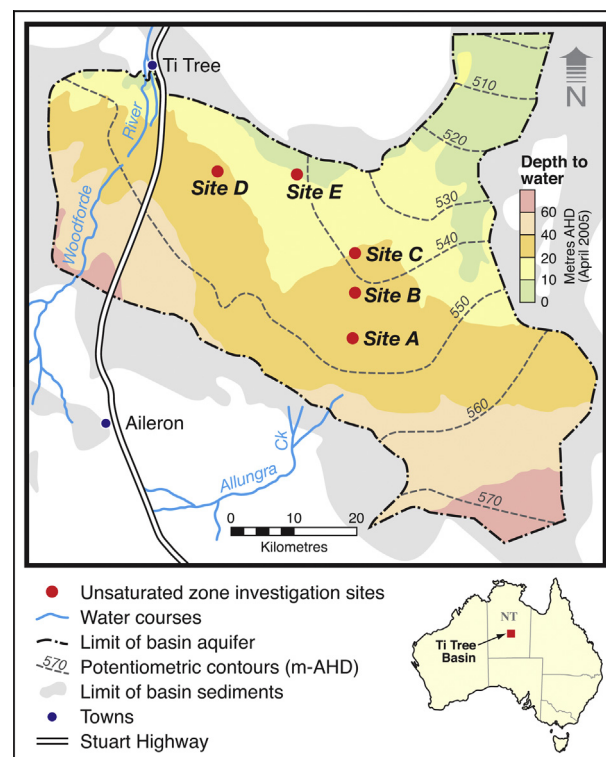

Fig. 1. Study sites in the Ti Tree Basin, Northern Territory, Australia.

watertable areas near the Woodforde River have historically shown rises in response to heavy rainfall and flooding, however there is little evidence that this has occurred since the year 2000, and groundwater levels are generally static or slightly declining at rates of 0.01–0.05 m yr^{-1} (Knapton, 2009). Total dissolved solids (TDS) of groundwater ranges from <1500 mg L^{-1} in the southern parts of the basin, but increases to >100,000 mg L^{-1} towards the northern terminus of the basin.

Harrington et al. (2002) investigated recharge processes in the basin using environmental tracers (chloride, carbon 14 and stable isotopes). Carbon 14 activities in groundwater ranged from 4 to 70 pMC, and groundwater ages were estimated using a geochemical correction scheme that accounted for addition of HCO$_3$ from weathering of old silicate minerals and calcite. The ^{14}C activity of soil gas was assumed to be 100 pMC. Estimated recharge rates from corrected groundwater ages ranged from 0.1 to 50 mm y^{-1} (median 0.9 mm y^{-1}), in reasonable agreement with the mean rate provided by the chloride mass balance method (0.8 mm y^{-1}). The higher recharge rates were spatially linked to the areas overlain by the (normally dry) Woodforde River and Allungra Creek floodplain. Hence across the Basin recharge is believed to be low, although higher recharge may occur during rare flood events in areas associated with surface water features (Harrington et al., 2002).

3. Methods

3.1. Methods – field programme

Installation of unsaturated zone gas samplers was concurrent with piezometer installation in the Ti Tree Basin between 2011 and 2012. Conventional rotary drilling methods were used with a blade bit and air circulation. Where hard calcrete and silcrete layers were encountered, a hammer bit was used. Piezometers were completed at five sites with 50 mm diameter PVC that had slotted screens of 1 mm aperture. For all piezometers, screen length was

between 1 and 2 m with a gravel pack (5–7 mm aggregate gravel) around the screen. Bentonite was used to seal the borehole annulus above the gravel pack and the remainder of the borehole was back filled to the surface with sand. Unsaturated zone gas sampling tubes consisted of ¼" nylon tubing fitted with a stainless steel filter on the end. These were taped to the outside of the piezometers during installation and a connection port was attached to the tubing at the ground surface. The filter ends of the gas sampling tubes served to prevent any soil particulate matter entering and potentially clogging the tubing, and were 'screened' in the backfill material (sand). At each site up to six gas sampling tubes of different length were attached to the outside of the piezometer, so that samples could be taken at multiple depths.

Samples of unsaturated zone gas were collected for analysis of CO_2 (percent by volume), ^{14}C (pMC), $\delta^{13}C$ (‰), CFC-11 and CFC-12 (pptv). Sampling was conducted in 2011 for sites A to E (Fig. 1). Unsaturated zone gas samples were collected by attaching a small air pump to the sampling ports at the surface. The pump was run for five minutes at a flow rate of $\sim$500 mL min^{-1} to flush the sampling tube then a sample was collected into either 110 ml Isotubes (^{14}C and $\delta^{13}C$ analysis) or 330 ml stainless steel canisters (CFC and CO_2 analysis). Groundwater was sampled from the piezometers to which the gas samplers were attached, using a Grundfos MP1 submersible pump. Samples were collected for carbon isotope analysis after approximately three bore volumes had been purged and field parameters (electrical conductance, pH, temperature) had stabilised, and stored in 1 L high density polyethylene plastic bottles.

Analysis of ^{14}C and $\delta^{13}C$ was performed on groundwater and unsaturated zone gas using the method described by Meredith et al. (2012), however acid evolution (to convert DIC to CO_2) was not required in the case of unsaturated zone gas. The analysis was performed using AMS facilities at the Australian Nuclear Science and Technology Organisation (ANSTO, Fink et al., 2004). ^{14}C activities of unsaturated zone gas and groundwater are reported as the ratio $^{14}CO_2$:$^{12}CO_2$ and $^{14}C_{DIC}$:$^{12}C_{DIC}$ (respectively) relative to the international standard (Stuiver and Pollach, 1977) in units of pMC. Stable isotope ratios (^{13}C:^{12}C) are reported in per mil (‰) relative to the international standard (Craig, 1957).

CO_2 analysis was performed at Flinders University, South Australia, using a Quibit S-151 CO_2 analyser. Given the relatively low range of the CO_2 analyser (0–2000 ppm), samples were diluted in a closed loop of known volume using ultra high purity (UHP) nitrogen and appropriate corrections applied to give an accurate measurement of CO_2 concentration. CFCs were analysed by gas chromatography at CSIRO Land and Water in Adelaide, South Australia, using a setup similar to that described by Busenberg and Plummer (1992). Only CFC-12 data is presented in this paper, as the trends in both tracers are well correlated.

3.2. Methods – modelling

Based on previous studies, dilution of unsaturated zone ^{14}C can be linked to production of CO_2 relatively devoid of ^{14}C, hence our modelling approach is to model both $^{14}CO_2$ and $^{12}CO_2$ production and transport in the unsaturated zone. Modelling $^{12}CO_2$ and $^{14}CO_2$ separately in identical units allows us to consider the ratio ^{14}C:^{12}C in soil gas for direct comparison to our measured units of ^{14}C activity (pMC). Following the work of Thorstenson et al. (1983), we converted ^{14}C activity in pMC to concentration units of $^{14}CO_2$ in mass/volume (mmol m^{-3}), and estimated $^{12}CO_2$ concentration (mmol m^{-3}) based on measurements of CO_2 (ppm) and the calculated $^{14}CO_2$ concentrations (knowing that ^{14}C in pMC directly relates to the ratio ^{14}C:^{12}C).

Our model considers advective and diffusive transport in the liquid phase and diffusive transport in the gaseous phase. Given the arid environment transport is predominantly diffusive in the

gas phase. We have constrained diffusive transport through measurement and modelling of CFCs. CFCs are trace gases of anthropogenic origin, which were introduced into the atmosphere in the 1950s. Their atmospheric concentration increased until the 1990s when they were phased out of production (owing to their ozone depleting qualities). Atmospheric concentrations have been measured in several locations, including Australia, over the past 60 years, hence input concentrations to the unsaturated zone over time are known. Therefore CFCs can be used to indicate timescales of unsaturated zone gas transport (Cook and Solomon (1995)) and help determine parameters related to the effective diffusion coefficient in a soil (e.g. porosity and tortuosity, Weeks et al., 1982).

To reproduce our data we modelled CFC-12, $^{12}CO_2$ and $^{14}CO_2$ using HYDRUS 1-D (Šimunek et al., 2013). HYDRUS uses the Richards equation to model variably saturated flow:

$$\frac{\partial \theta}{\partial t} = \frac{\partial}{\partial x}\left(K\left(\frac{\partial h}{\partial x} + \cos \alpha \right) \right) - S \tag{1}$$

where θ is volumetric water content (m^3 m^{-3}), h is the water pressure head (m), t is time (y), x is the spatial coordinate (m), K is the unsaturated hydraulic conductivity (m y^{-1}), α is the angle between the flow direction and the vertical axis (0° for vertical flow in our case) and S is the sink term. Solute transport is modelled with an advection dispersion equation in which transport may occur in the liquid and gas phases. Exchange between the liquid and gas phase is assumed to be instantaneous and determined by the partition coefficient:

$$k_g = \frac{c_w}{c_g} \tag{2}$$

where c_w and c_g are concentrations in the liquid and gas phase (mmol m^{-3}). We assume that sorption is negligible for both CFCs (Cook and Solomon, 1995) and CO_2, hence there is no partitioning between the solid and liquid phases. Sorption of $^{14}CO_2$ may become important as water content increases (Striegl and Armstrong, 1990), however preliminary modelling showed our results to be insensitive to sorption at the low water contents we model. Thus the solute transport equation can be written as:

$$\frac{\partial \theta c_w}{\partial t} + \frac{\partial a_v c_g}{\partial t} = \frac{\partial}{\partial x}\left(\theta D^w \frac{\partial (c_w)}{\partial x} \right) + \frac{\partial}{\partial x}\left(a_v D^g \frac{\partial c_g}{\partial x} \right) - \frac{\partial q c_w}{\partial x}$$
$$- \lambda \theta c_w - \lambda a_v c_g + \gamma c_g a_v \tag{3}$$

where q is the volumetric flux (m y^{-1}); λ is the decay constant for ^{14}C (y^{-1}), γ represents production of CO_2 in the gas phase (mmol m^{-3} y^{-1}), a_v is the air content (m^3 m^{-3}), D_w is the dispersion coefficient in the liquid phase (m^2 y^{-1}) and D^g is the diffusion coefficient in the gas phase (m^2 y^{-1}). The diffusion coefficients are calculated as follows:

$$D^W = D_L \frac{|q|}{\theta} + \theta D_0^W \tau_W \tag{4}$$

$$D^g = a_V D_0^g \tau_g \tag{5}$$

where D_L is longitudinal dispersivity (m), $|q|$ is the absolute value of the volumetric water flux (m y^{-1}), D_0^W is the molecular diffusion coefficient of the solute in free water (m^2 y^{-1}) and τ_w is tortuosity for the liquid phase (–); D_0^g is the molecular diffusions coefficient in free air and τ_g is tortuosity in the gas phase (–). Tortuosity is calculated within the model based on water and air content in the liquid and gas phase using the relationships derived by Millington and Quirk (1961):

$$\tau_W = \frac{\theta^{\frac{7}{3}}}{\theta_S^2} \tag{6}$$

$$\tau_g = \frac{a_V^{\frac{7}{3}}}{\theta_S^2} \tag{7}$$

where θ_s is the saturated water content (equivalent to total porosity).

The models are 1D columns which represent the full extent of both the unsaturated and saturated zones at each site, however only transport in the unsaturated zone is of interest here (as ^{14}C activities in groundwater will be influenced by up-gradient processes, and cannot be accurately considered in 1D). The Van Genuchten (1980) model for soil hydraulic properties was used. However as the models are run with steady state flow and water content does not vary with time, the model results are insensitive to the hydraulic model used. The models were finely discretised at the surface (cells of 0.05 m thickness), with increasing cell thickness with depth to a maximum of 0.5 m.

The upper boundary condition for flow was a second type boundary which allows for a specified recharge flux into the model. The upper boundary condition for solutes was a specified concentration boundary. A transient upper concentration boundary condition for CFC-12 was based on atmospheric measurements in the southern hemisphere from 1952 to 2012 (CSIRO, 2013). A constant upper concentration boundary for the $^{12}CO_2$ and $^{14}CO_2$ models was based on concentrations for a carbon 14 activity of ~108 pMC and a ^{14}C:^{12}C ratio of 1.39×10^{-12} estimated from data in Hua et al. (2013). The activity of 108 pMC was chosen as it appears to be consistent with the uppermost values in the unsaturated zone at our sites (from plant respired CO_2). Although the ^{14}C activity of atmospheric CO_2 has changed over the timescale of our model we do not model this, as Thorstenson et al. (1983) have previously shown that such a transient ^{14}C atmospheric boundary condition does not have a significant influence on the unsaturated zone profile.

The lower boundary for flow was a first type boundary, which was assigned by setting a pressure head boundary (m) at the bottom of the model domain, with an appropriate pressure head value to represent the watertable depth (this establishes the unsaturated/saturated interface). This boundary was made constant so that the position of the watertable does not change with time regardless of recharge fluxes across it. The lower boundary conditions for concentration were set at zero to represent infinite age at the bottom of the profile.

An initial model was run to steady state with zero recharge to establish initial flow conditions, then the CFC model was calibrated (to constrain gas transport parameters). The model for CFC-12 was run for 60 years representing the period over which atmospheric CFCs have been above zero. Diffusion coefficients in free air and water (D_0^W and D_0^g) were based on literature values (Table 1). Given that tortuosity is determined within the model and water contents are likely to be low, calibration was achieved manually by altering porosity (which informs the values for a_v and θ_s and hence the effective diffusion coefficients D^g and D^w).

The porosity values determined by the CFC modelling were then used to model $^{12}CO_2$ and $^{14}CO_2$ profiles (with appropriate free air and water diffusion coefficients D_0^W and D_0^g for both species, Table 1). Calibration of the CO_2 models was achieved manually by altering production rates in (a) the top 10 m for both $^{12}CO_2$ and

$^{14}CO_2$ models – replicating respiration of modern CO_2 by plant roots (based on observations of atmospheric ^{14}C at this depth, and knowledge of the vegetation types in the area (O'Grady et al., 2009)) and (b) in a 2 m thick zone above the watertable for the $^{12}CO_2$ model only, replicating production of CO_2 devoid of $^{14}CO_2$. The ratio of modelled $^{14}CO_2$:$^{12}CO_2$ was then calculated and compared to our measurements of ^{14}C activity as a final check on the model fit.

A number of scenarios were run in order to further our understanding of unsaturated zone processes and their influence on ^{14}C activity. We modelled profiles with a variety of watertable depths (12–100 m) and varied recharge rates from 0 to 500 mm y^{-1}. We also varied the rate and thickness of shallow atmospheric CO_2 production (100–10,000 mmol m^{-3} y^{-1}) to assess the influence of root respiration and root depth. These rates of CO_2 production correspond to rates of soil respiration of 0.3–32 mol m^{-2} y^{-1}, which equate to carbon fluxes of 3.6–384 g C m^{-2} y^{-1}. This covers the range for arid areas reported by Raich and Schlesinger (1992) of 60–224 g C m^{-2} y^{-1} (based on limited measurements). Rates of deep 'old' CO_2 production were also varied (0–500 mmol m^{-3} y^{-1}). There are few reported rates of shallow/deep CO_2 production in the literature that pertain to this problem. Keller and Bacon (1998) and Walvoord et al. (2005) give deep production rates of 47 and 100 mmol m^{-3} y^{-1} respectively, hence our scenarios cover this range.

4. Results

4.1. Results – field data

Fig. 2 shows measured concentrations of ^{14}C (pMC) CFC-12 (pptv), CO_2 (percent by volume) and δ^{13}C (‰) in unsaturated zone gas at each site. ^{14}C activities in groundwater sampled below these profiles (generally within 2–6 m of the watertable, however at Site D the groundwater sample is from 18 m below the watertable) are also shown in Fig. 2. Measurement errors are not shown as they are generally very low (±5% for CFCs and CO_2, ± <1% for ^{14}C). ^{14}C activities are generally modern (>100 pMC) within the top 11 m of each profile and decline relatively uniformly with depth, with variable watertable depths leading to varying ^{14}C activities directly above the watertable. The exception is Site C which shows a sharp decline in ^{14}C activity to 54 pMC in a shallower profile than Site A and B. The shallowest site (E) shows modern ^{14}C throughout the profile to a depth of 8.2 m.

The modern ^{14}C activity and high CO_2 in the top 11 m of each profile suggests a modern source of CO_2 is present. The most likely source of this modern CO_2 is plant root respiration rather than the oxidation of organic matter, as a significant amount of modern organic matter is unlikely to be present at depths up to 11 m in this arid setting (Trumbore, 1993). Also the presence of tree roots to depths of 11 m in this type of environment is not unrealistic (O'Grady et al., 2009), and the δ^{13}C results fall in a relatively narrow range of −13.5 to −16.8‰, which is around the

Table 1
Diffusion and partition coefficients used for models shown in Fig. 3.

Parameter	Value	Reference
CFC-12 diffusion coefficient in air (D_0^g), m^2 y^{-1}	287	Montfort and Pellegatta (1991)
CFC-12 diffusion coefficient in water (D_0^W), m^2 y^{-1}	3.41×10^{-2}	Zheng et al. (1998)
CFC-12 partition coefficient (k_g)	0.0718	Warner and Weiss (1985)
$^{14}CO_2$ diffusion coefficient in air (D_0^g), m^2 y^{-1}	515	Walvoord et al. (2005)
$^{12}CO_2$ diffusion coefficient in air (D_0^g), m^2 y^{-1}	520	Walvoord et al. (2005)
CO_2^* diffusion coefficient in water (D_0^W), m^2 y^{-1}	6.03×10^{-2}	Jahne et al. (1987)
CO_2 partition coefficient (k_g)	0.836	Weiss (1974)

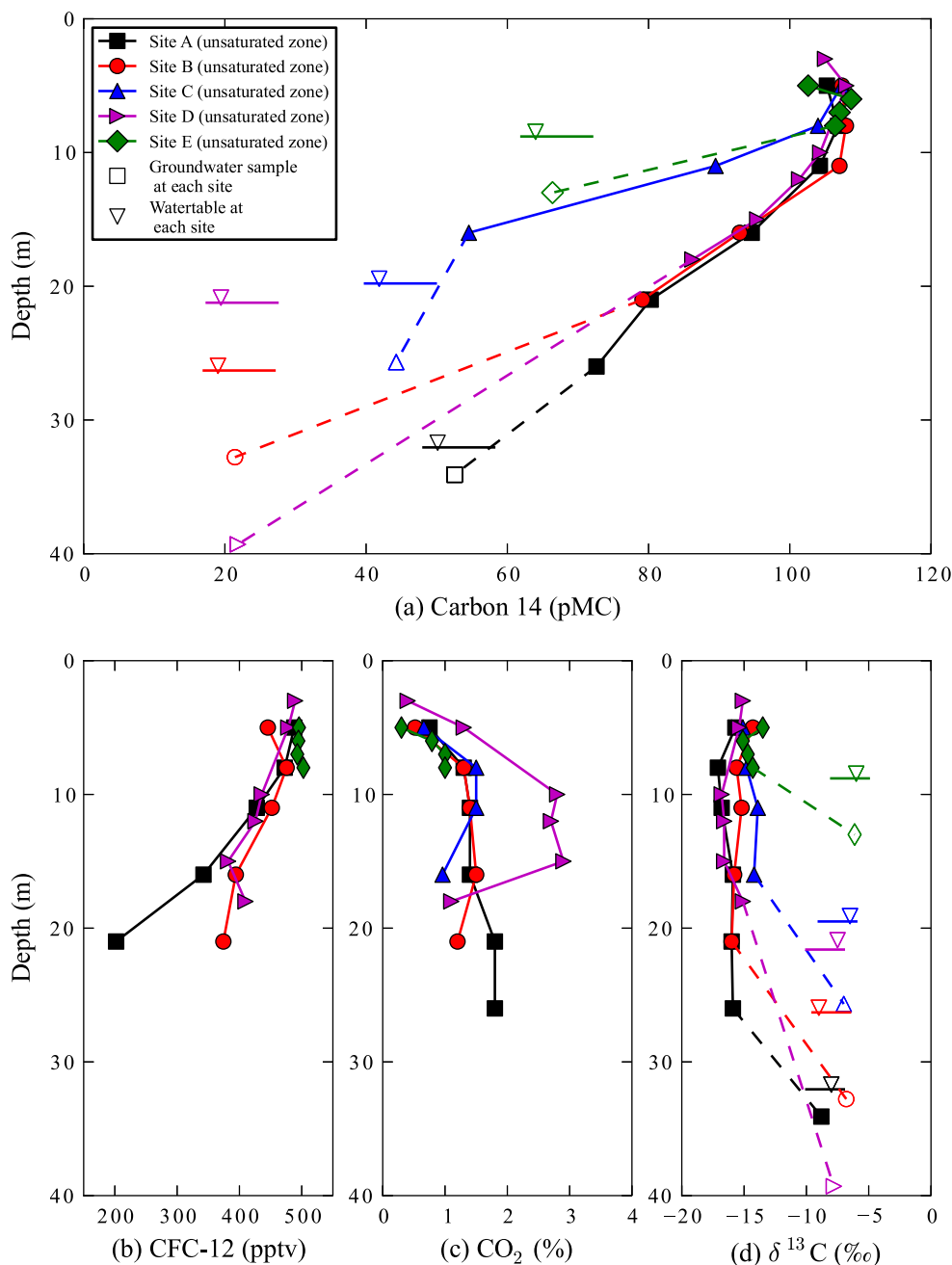* The same diffusion coefficient in water D_0^W was applied to both $^{12}CO_2$ and $^{14}CO_2$.

Fig. 2. Measured concentrations of (a) ^{14}C, (b) CFC-12, (c) CO_2 and (d) δ^{13}C in unsaturated zone gas in the Ti Tree Basin. ^{14}C activities in groundwater beneath these profiles are also shown.

values that would be expected from respiration from spinifex grass (~−14‰, Cook and Dawes-Gromadzki, 2005).

The similarity in declines of ^{14}C activity with depth at Sites A, B and D suggest that the mechanisms responsible for ^{14}C dilution are relatively consistent throughout the study area. We have not investigated the mechanism for this dilution in great detail, however the presence of soft and cemented calcrete above and below the watertable at our sites suggests the source of 'old' CO_2 is similar to that identified by Walvoord et al. (2005). That is, precipitation of calcite at the watertable (in the case of Walvoord et al. promoted by a slowly declining watertable) releases old CO_2 via:

$$Ca^{2+}_{(aq)} + 2HCO^{-}_{3(aq)} \leftrightarrow CO_{2(g)} + H_2O_{(l)} + CaCO_{3(s)} \qquad (8)$$
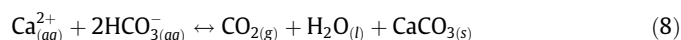
At Site C, ^{14}C appears more depleted and the trend with depth is different to the other sites. Drilling logs from this site revealed significantly more calcrete in the profile, commencing at 6 m depth (13 m above the watertable). This calcrete may act as a source of old CO_2 through active dissolution–precipitation reactions in this shallower part of the profile, with precipitation (and release of CO_2) possibly driven by evapotranspiration of shallow soil water (Dever et al., 1987). However understanding the physical drivers for calcite precipitation at our site would require further work and was beyond the scope of this study.

CFC-12 concentrations are close to current atmospheric concentrations (~525 pptv, CSIRO, 2013) in the upper parts of the profiles and then decrease with depth towards the watertable, consistent with existing theory on CFC transport in the unsaturated zone

(Cook and Solomon, 1995). The CFC-12 concentrations at the bottom of the profiles represent apparent lag times (time taken for diffusive transport from the surface to the base of the profile) of 35 years for Site A (depth to water of 31.5 m), 25 years for Site B and D (watertable depths of 25.8 m and 20.6 m respectively) and 18 years for Site E (depth to water of 8.2 m). CO_2 concentrations are much higher (up to 60 times higher) than atmospheric concentrations (~393 ppm at the time of the study, CSIRO, 2013) and generally increase with depth. Concentrations are highest at site Site D from 10 to 15 m depth before declining towards the watertable. We cannot explain this decline in terms of any physical process and hence it is likely the low concentration near the watertable represents contamination from loss to the atmosphere either in sampling, sample transport or analysis. ^{14}C samples do not appear to show any contamination though, and the trend of declining activity is present.

4.2. Results – modelling of field data

Fig. 3 shows modelling results from the deepest profile (Site A). Porosity, $^{12}CO_2$ and $^{14}CO_2$ production rates that provided the best model fit, as well as other model parameters are given in Table 2. The best fit to CFC-12 data was obtained with a porosity of 0.4 in the top 10 m of the profile, and 0.2 from 10 m to the watertable. The higher porosity (and hence higher effective diffusion coefficient) required in the upper layers of the model may have several causes other than changes in soil texture, such as the presence of root channels and animal burrows. This also captures likely higher rates of effective gas diffusivity in the shallow unsaturated zone which may be driven by barometric pumping (Weeks et al., 1982). Since HYDRUS relates tortuosity to water and air content (Eqs. (6) and (7)), changing porosity is the only way to change the effective diffusion coefficients (Eqs. (4) and (5)) to accurately simulate the CFC transport. The best fit to carbon isotope profiles at Site A was achieved with $^{12}CO_2$ production rates of 863 mmol m^{-3} y^{-1} in the upper 10 m (accompanied by $^{14}CO_2$ production of 1.2×10^{-9} mmol m^{-3} y^{-1} based on the atmospheric ratio) and 290 mmol m^{-3} y^{-1} in a 2 m thick zone above the

watertable (with no accompanying $^{14}CO_2$ production). $^{12}CO_2$ flux out of the top of the calibrated model (i.e. modelled soil respiration) was ~3 mol m^{-2} y^{-1}.

All other sites were likewise modelled and Fig. 4 shows the calibrated ^{14}C (pMC) profiles. The goodness of fit varies but the profiles are mostly well matched, with the decrease in ^{14}C activity replicated in the models. Shallow production rates (0–10 m) varied from 600 to 1500 mmol m^{-3} y^{-1}, while deep production rates varied from 290 to 450 mmol m^{-3} y^{-1} (in a 2 m thick zone above the watertable), reflecting the range in CO_2 concentrations observed (Fig. 2(c)). The shallowest profile (8.2 m depth) was modelled without a deep source of old CO_2 as measured $^{14}CO_2$ activity was modern for the entire profile suggesting no significant source of old CO_2. Soil respiration rates, determined from the model as the concentration flux out of the top boundary of the soil profile, ranged from 0.9 to 3.3 mol m^{-2} y^{-1} (Table 2 summarises this information for each profile). Our modelled soil respiration rates are relatively low compared with carbon flux values measured by eddy covariance (EC) towers in the Ti Tree Basin (up to 59 mol m^{-2} y^{-1}, Cleverly et al., 2013). However these measurements include CO_2 flux from vegetative respiration and photodegradation of organic matter, which Cleverly et al. (2013) cite as much larger sources of CO_2 flux than soil respiration. Our values of soil respiration do however compare well with modelled values from both Keller and Bacon (1998) and Walvoord et al. (2005) of 2.9 mol m^{-2} y^{-1} and 3 mol m^{-2} y^{-1} respectively.

4.3. Results – sensitivity analysis

The purpose of the scenario modelling was to assess the sensitivity of ^{14}C activity in the unsaturated zone to changes in the calibrated parameters (shallow and deep production rate and thickness of production zones) as well as the influence of watertable depth and recharge rate. Fig. 5 shows the influence of different $^{12}CO_2$ and $^{14}CO_2$ production rates and production zone thicknesses on the modelled ^{14}C (i.e. the ratio of modelled $^{14}CO_2$ to modelled $^{12}CO_2$) for Site A. Low rates of shallow atmospheric CO_2 production result in greater dilution of ^{14}C with depth (5a)
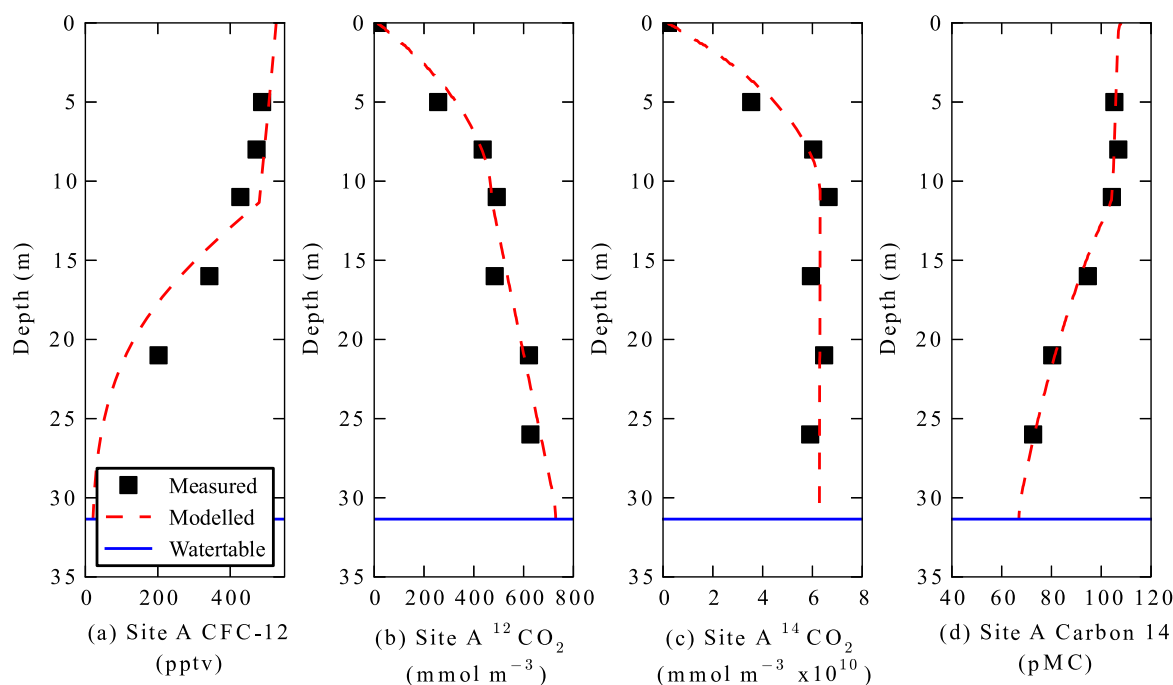
Fig. 3. Measured and modelled concentrations of CFC-12, $^{12}CO_2$, $^{14}CO_2$ and ^{14}C activity (as pMC) for Site A.

Table 2
Summary of CO_2 production rates and porosity values used to calibrate each model.

Site	Site A	Site B	Site C	Site D	Site E
Piezometer registration number (RN)	18611	18779	18781	18893	18897
Depth to water (m-bgl)	31.5	25.8	19.1	20.6	8.2
Shallow $^{12}CO_2$ production rate (mmol m^{-3} y^{-1})	863	1007	863	1500	600
Deep $^{12}CO_2$ production rate (mmol m^{-3} y^{-1})	290	300	400	450	–
Modelled soil respiration rate (mol m^{-2} y^{-1})	2.8	3.3	1.7	3.9	0.9
Porosity	0–10 m: 0.4	0–10 m: 0.4	0–10 m: 0.35	0–10 m: 0.33	0–5 m: 0.28
	10–31.5 m: 0.2	10–23 m: 0.35	10–19.1 m: 0.2	10–15 m: 0.27	5–8.2 m: 0.35
		23–25.8 m: 0.2		15–20.6 m: 0.38	
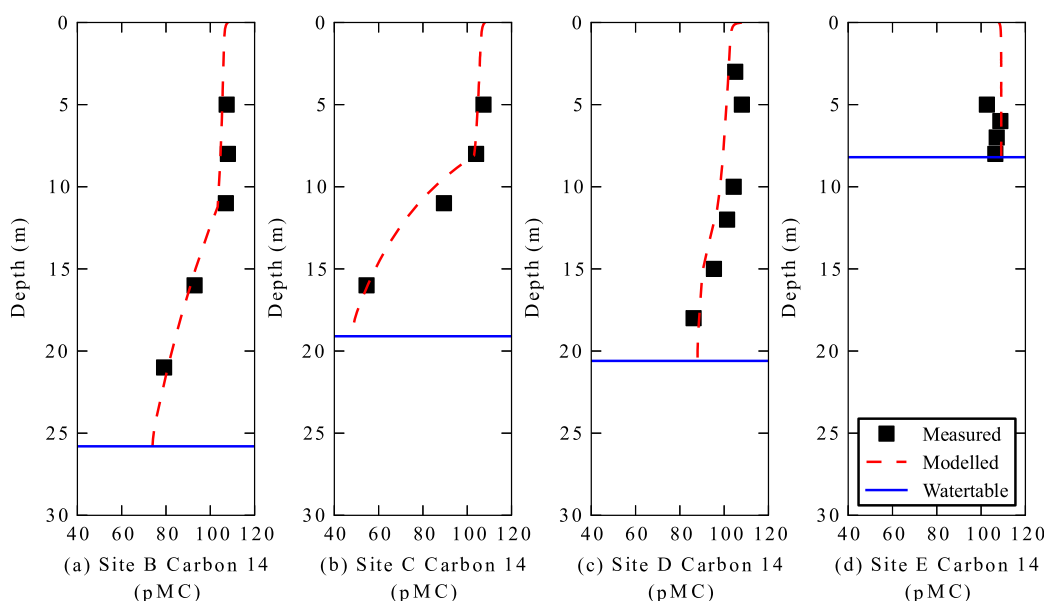
Fig. 4. Calibrated ^{14}C (pMC) models for all other profiles.

as there is less 'modern' CO_2 in the profile to buffer against the production of 'old' CO_2. Similarly, lower rates of deep 'old' CO_2 production result in less dilution of ^{14}C and activities are higher with depth (5b), consistent with the sensitivity modelling performed by Walvoord et al. (2005).

The thickness of the deep production zone is relatively unimportant, so long as the total CO_2 production rate is the same. However the same cannot be said for the thickness of the shallow zone of modern CO_2 production. Panel (5d) shows that shallower zones of modern CO_2 production (with the same total amount of soil respiration) result in greater dilution of ^{14}C above the watertable. This is because with a smaller zone of modern CO_2 production there is less ^{14}C present with depth, and the profile becomes dominated by upward diffusion of the deep, older $^{12}CO_2$ (diluting the ^{14}C activity). A greater amount of modern CO_2 needs to be produced when the root zone is shallower in order to avoid this dilution. For example, modelling Site A with a 5 m thick root zone meant a $^{12}CO_2$ production rate of 10,000 mmol m^{-3} y^{-1} (i.e. ten times greater than that used in the calibrated model with a 10 m thick root zone) was needed to produce the same profile of dilution of ^{14}C. This however resulted in $^{12}CO_2$ and $^{14}CO_2$ models that show concentrations that are much higher than measured values in the top 5 m. It should be noted that in Panel (5d), the higher porosity (0.4) is maintained in the top 10 m for all scenarios except where the root zone is extended to 15 m – here the porosity is also higher to 15 m. This explains the inflection point in the graph seen at 15 m.

Fig. 6 shows the influence of recharge (6a), shallow CO_2 production (6b), deep CO_2 production (6c) and root depth (6d) on the ^{14}C activity of unsaturated zone gas above the watertable for various watertable depths. In all these scenarios, parameters are held con-

stant at the values used to calibrate Site A (Fig. 3; Table 2) except for those parameters being tested as shown in each panel. The first apparent conclusion is that when watertables are deeper there is more depletion of ^{14}C with depth for nearly all scenarios considered. This is consistent with our field measurements which showed similar trends in ^{14}C activity with depth, but varying activities at the watertable as dictated by the variation in watertable depth.

Fig. 6(a) shows that when recharge is low (1–10 mm y^{-1}), there is no significant change in ^{14}C above the watertable. As recharge increases there is less dilution of ^{14}C activity above the watertable (because there is more advective transport of $^{14}CO_2$ downwards), however this effect is most significant when the watertable is deeper. For example for recharge rates of 1–100 mm y^{-1}, the ^{14}C activity of gas above the watertable varies from 22 to 45 pMC when the depth to water is 100 m, but only varies from 51 to 62 pMC when the depth to water is 40 m. When recharge is very high (>300 mm y^{-1}) there is less dilution of ^{14}C, with values generally >80 pMC.

The influence of shallow 'modern' CO_2 production on ^{14}C activity of unsaturated zone gas above the watertable can be seen in Fig. 6(b). As with the model for site Site A, modern CO_2 production is limited to the top 10 m of the unsaturated zone, deep production is limited to a 2 m thick zone above the watertable (with the deep production rate kept constant at 290 mmol m^{-3} y^{-1} for each scenario) and recharge is 0 mm y^{-1}.

Fig. 6(c) shows the modelled influence of deep $^{12}CO_2$ production. Shallow $^{12}CO_2$ and $^{14}CO_2$ production is kept constant and recharge is 0 mm y^{-1}. Greater rates of deep $^{12}CO_2$ production result in greater dilution of ^{14}C. When there is no deep CO_2 production however, there is no significant dilution of ^{14}C above the water-
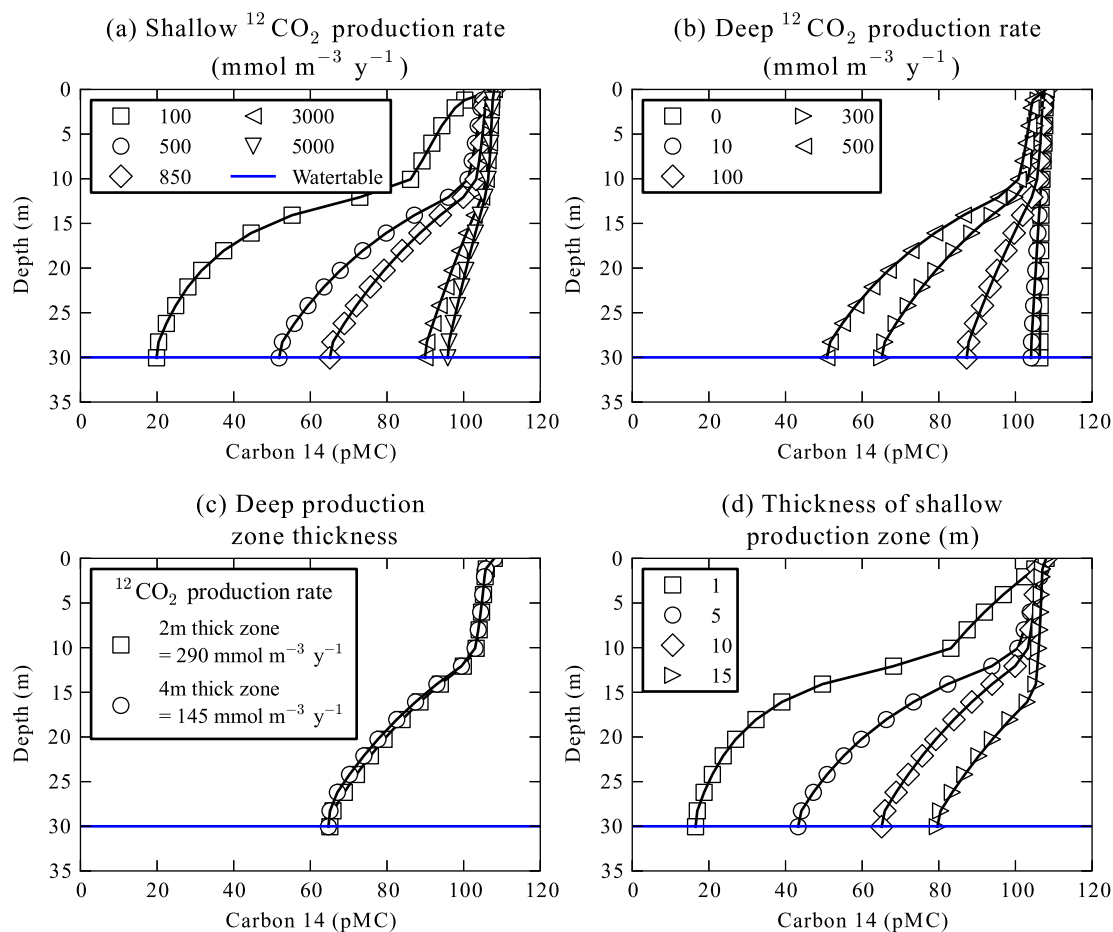
Fig. 5. Influence of (a) shallow and (b) deep rate of $^{12}CO_2$ production for Site A. Panel (c) shows that the thickness of the zone of deep CO_2 production is relatively unimportant so long as bulk CO_2 production is the same however panel (d) shows that the thickness of the shallow production zone is important.

table, even when the depth to water is 100 m. Fig. 6(d) shows that the thickness of the zone of shallow 'modern' CO_2 production is significant in influencing the ^{14}C activity of unsaturated zone gas. As discussed earlier this is because the production of deep 'old' CO_2 starts to dominate the profile when 'modern' CO_2 is closer to the surface (and diffuses out more rapidly).

5. Discussion

Both our data and our model support the hypothesis that ^{14}C in unsaturated zone gas above the watertable is controlled primarily by stratified production of CO_2 from isotopically different sources. This is consistent with previous work on unsaturated zone ^{14}C measurements (Keller and Bacon, 1998; Walvoord et al., 2005). Our results extend these earlier findings to show that these processes can be relatively consistent across large areas in a groundwater basin, but that variation in watertable depth may lead to spatial variability in the ^{14}C activity of unsaturated zone gas directly above the watertable.

The scenario modelling in this study helps elucidate the conditions under which depletion of unsaturated zone ^{14}C may become significant for ^{14}C dating of groundwater. We find that depletion of ^{14}C may be more significant where watertables are deeper (>10 m). The degree to which ^{14}C is depleted above the watertable is not affected by low rates of recharge (0–10 mm y^{-1}). However it is sensitive to both the shallow CO_2 production rate and the thickness of this production zone (root zone thickness), with lower rates of

shallow CO_2 production ($^{12}CO_2$ and $^{14}CO_2$) leading to greater depletion. This helps explain some of the different profiles seen in previous studies. For example Leaney and Allison (1986) observe high ^{14}C activity (>90 pMC) to depths of 35 m in the unsaturated zone in an area where mallee vegetation is known to be very deep rooted (roots extending to 15–20 m depth, Cook et al. (1989)). However Keller and Bacon (1998) observe significant dilution of ^{14}C in a 7 m deep profile, where the root zone is only 1 m thick. Higher rates of deep 'old' CO_2 production ($^{12}CO_2$ only) likewise lead to greater depletion. Recharge is generally lower and more sporadic in arid areas (Scanlon et al., 2006), which suggests that the dilution of ^{14}C activity in unsaturated zone CO_2 may be more of a problem in arid areas, and most previous studies of unsaturated zone ^{14}C come from arid areas. However the root depth of vegetation in arid areas may be significant (>20 m, Canadell et al., 1996) which would potentially limit the amount of dilution as Fig. 6(d) shows, presuming such deep roots are respiring atmospheric CO_2. Therefore determining if there is dilution of ^{14}C in unsaturated zones on a site by site basis would require a broad understanding of the local hydrogeology (recharge rates) and ecology (rooting depth). Variations in soil type will also become important, with lower porosity soils having lower diffusion coefficients, hence potentially more depletion of ^{14}C activity at depth, however we have not assessed this in our sensitivity analysis. Nevertheless, for general purposes when watertables are deep, recharge is moderate to low and vegetation rooting does not extend to the watertable, ^{14}C in the unsaturated zone may be significantly diluted if a source of old CO_2 is present. The presence of organic matter or
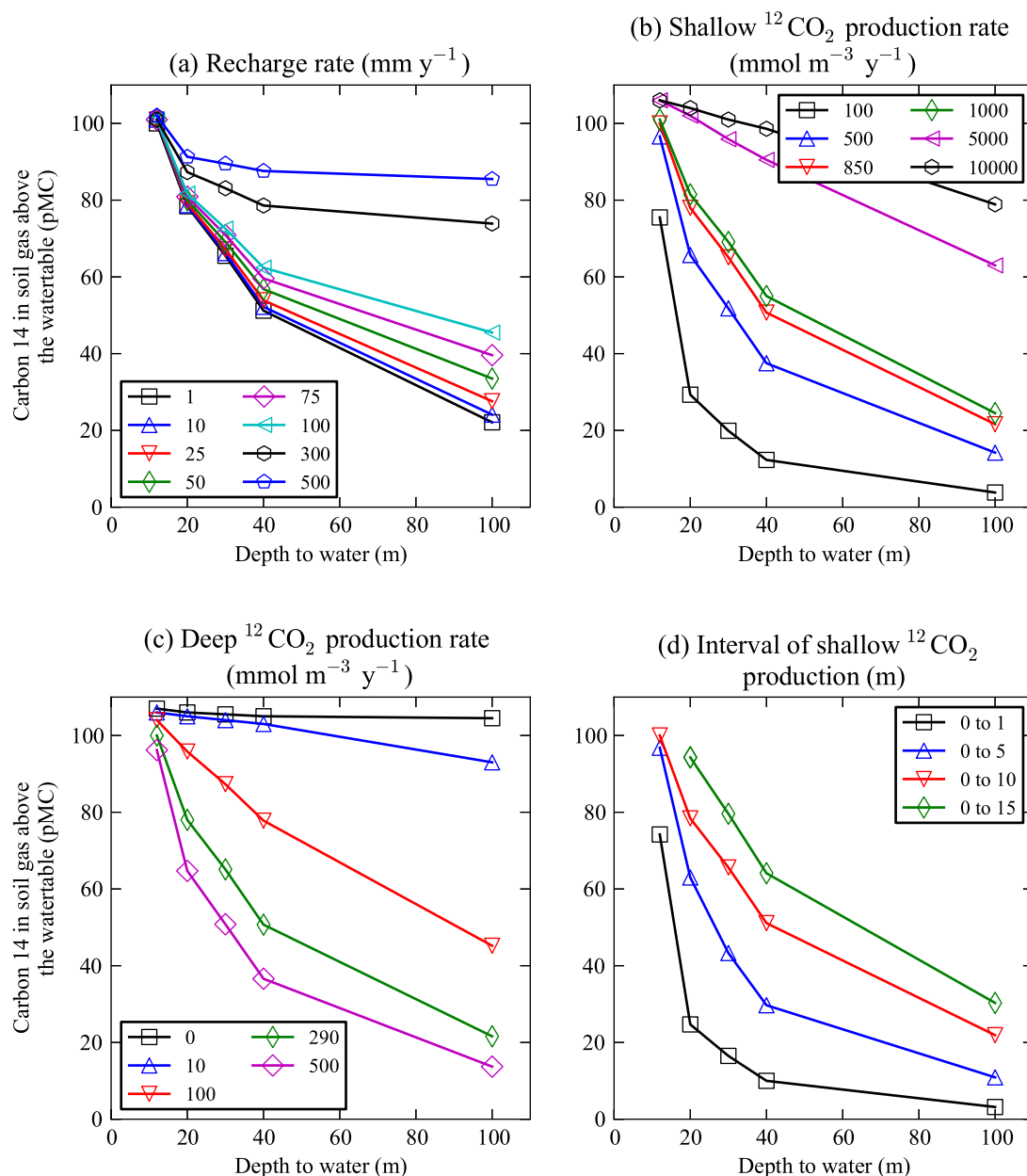
Fig. 6. Modelled results from Hydrus showing the influence of (a) recharge rate, (b) shallow CO_2 production, (c) deep CO_2 production and (d) the depth of the shallow CO_2 production zone (i.e. depth of root zone) on calculated ^{14}C activity (pMC) of unsaturated zone gas directly above the watertable (for DTW 12–100 m).

minerals within the aquifer such as calcite should also act as an indicator as to when unsaturated zone ^{14}C may be diluted.

Our model assumes steady state flow and production, however both recharge and root respiration will vary temporally. However previous studies have shown that transient variation in shallow unsaturated zone CO_2 does not necessarily influence variations in ^{14}C, and that ^{14}C activities of unsaturated zone CO_2 are controlled by other processes such as the ones considered in this paper (Thorstenson et al., 1983; Bacon and Keller, 1998). Episodic recharge, driven by rare and extreme rainfall events, is likely to be an important recharge mechanism in Ti Tree. Hydrographs from some bores in the Basin show sporadic sharp rises in water level, indicating episodic recharge has occurred at least five times in the last 50 years, with the last event in the year 2000 (Knapton, 2009). However this does not seem to have affected CFC profiles, with apparent gas ages of up to 35 years (i.e. equivalent of atmospheric concentrations in 1976) at depth, suggesting episodic

recharge events of the magnitude observed in Ti Tree do not 'flush' the unsaturated zone or perturb the unsaturated zone gas profiles significantly.

We did not measure the isotopic content of sedimentary organic carbon in our profiles which limits the interpretation of causes of CO_2 production in the unsaturated zone. However the assumption that production of CO_2 in the top 10 m at our site is from root respiration with a modern ^{14}C signature is likely given what is known about rooting depth of vegetation such as spinifex (Reid et al., 2008). We treat this root respiration in our model as being uniform with depth based on our CO_2 and ^{14}C measurements, however this assumption may not carry to all environments. We have not investigated organic carbon processes thoroughly as it was beyond the scope of this study, however other studies are furthering this work (Meredith et al., 2013). Likewise our understanding of the source of deep 'old' CO_2 is limited. Two mechanisms of deep CO_2 production in the unsaturated zone that

have been put forward in the literature are oxidation of organic matter (Keller and Bacon, 1998), and calcite precipitation (Walvoord et al., 2005). Given the absence of any significant organic matter in the lithology in Ti Tree and the presence of calcrete layers, we postulate that calcite precipitation is a source of old CO_2 in our case. However the mechanisms behind this are poorly understand, and it is not clear whether a slowly declining watertable is a pre-condition for calcite precipitation (Walvoord et al., 2005) or whether precipitation is independent of this. More work is needed to better understand the mechanisms for deep CO_2 production in different situations and settings. Further studies and measurement of unsaturated zone ^{14}C activity in different settings would benefit not only interpretation of groundwater age, but also understanding of these CO_2 production mechanisms.

6. Conclusion

Depletion of ^{14}C in unsaturated zone gas is a common occurrence based on the limited amount of published measurements available worldwide. This casts doubt on the typical assumption in ^{14}C dating of groundwater that unsaturated zone gas is in equilibrium with the atmosphere. Our measurements of unsaturated zone ^{14}C activity in the Ti Tree Basin support this finding for watertable depths >10 m. We have modelled depletion of ^{14}C in unsaturated zone gas with a shallow and deep source of CO_2 production from sources that have isotopically different signatures. We find that the processes controlling ^{14}C dilution in the unsaturated zone are relatively consistent over a large spatial area (distances of 35 km between sites), and that variation in watertable depth over this scale leads to spatial variation in ^{14}C activities directly above the watertable. It appears from our sensitivity analysis that the problem of ^{14}C dilution in the unsaturated zone may be more pronounced in arid settings (where recharge rates are lower), however further work is required to better understand the mechanisms of deep, old CO_2 production.

These findings improve our understanding of how unsaturated zone processes affect the spatial variation in ^{14}C activities directly above the watertable, with unsaturated zone depth being a key influence. This gives improved guidance as to when depletion of unsaturated zone ^{14}C becomes significant, which will be of great benefit for future researches looking to accurately determine groundwater ages from ^{14}C measurements.

Acknowledgements

References

Bacon, D.H., Keller, C.K., 1998. Carbon dioxide respiration in the deep vadose zone: implications for groundwater age dating. Water Resour. Res. 34 (11), 3069–3077.

Busenberg, E., Plummer, L.N., 1992. Use of chlorofluorocarbons (CCl_3F and CCl_2F_2) as hydrologic tracers and age dating tools: the alluvium and terrace system of central Oklahoma. Water Resour. Res. 28 (9), 2257–2283.

Canadell, J., Jackson, R.B., Ehleringer, J.R., Mooney, H.A., Sala, O.E., Schulze, E.D., 1996. Maximum rooting depth of vegetation types at the global scale. Oecologica 108, 583–595.

Cleverly, J.R., Boulain, N.P., Villalobos-Vega, R., Grant, N., Faux, R., Wood, C., Cook, P., Yu, Q., Leigh, A., Eamus, D., 2013. Dynamics of component carbon fluxes in a semi-arid Acacia woodland, central Australia. J. Geophys. Res.: Biogeosci. 118, 1–18.

Cook, G.D., Dawes-Gromadzki, T.Z., 2005. Stable isotope signatures and landscape functioning in banded vegetation in arid-central Australia. Landscape Ecol. 20, 649–660.

Cook, P.G., Solomon, D.K., 1995. Transport of atmospheric trace gases to the watertable: implications for groundwater dating with chlorofluorocarbons and krypton 85. Water Resour. Res. 31 (2), 263–270.

Cook, P.G., Walker, G.R., Jolly, I.D., 1989. Spatial variability of groundwater recharge in a semiarid region. J. Hydrol. 111, 195–212.

Craig, H., 1957. Isotopic standards for carbon and oxygen correction factors for mass-spectrometric analysis of carbon dioxide. Geochim. Cosmochim. Acta 12, 133–149.

CSIRO, 2013. Key greenhouse and ozone depleting gases, viewed January 2013. <http://www.cmar.csiro.au/research/capegrim_graphs.html>.

Dever, L., Fontes, J.C., Riche, G., 1987. Isotopic approach to calcite dissolution and precipitation in soils under semi-arid conditions. Chem. Geol. 66, 307–314.

Fink, D., Hotchkis, M., Hua, Q., Jacobsen, G., Smith, A.M., Zoppi, U., Child, D., Mifsud, C., van der Gaast, H., Williams, A., Williams, M., 2004. The ANTARES AMS facility at ANSTO. Nucl. Instrum. Methods Phys. Res. B 223–224, 109–115.

Fontes, J.C., Garnier, J.M., 1979. Determination of the initial ^{14}C activity of the total dissolved carbon: a review of the existing models and a new approach. Water Resour. Res. 15 (2), 399–413.

Haas, H., Fisher, D.W., Thorstenson, D.C., Weeks, E.P., 1983. $^{13}CO_2$ and $^{14}CO_2$ measurements on soil atmosphere sampled in the sub-surface unsaturated zone in the Western Great Plains of the US. Radiocarbon 25 (2), 301–314.

Harrington, G.A., Cook, P.G., Herczeg, A.L., 2002. Spatial and temporal variability of ground water recharge in central Australia: a tracer approach. Ground Water 40 (5), 518–528.

Herczeg, A.L., Leaney, F.W., 2011. Review: environmental tracers in arid-zone hydrology. Hydrogeol. J. 19, 17–29.

Hua, Q., Barbetti, M., Rakowski, A.J., 2013. Atmospheric radiocarbon for the period 1950–2010. Radiocarbon 55 (2), 1–14.

Ingerson, E., Pearson, F.J., 1964. Estimation of age and rate of motion of groundwater by the 14C-method. Recent Researches in the Fields of Atmosphere, Hydrosphere, and Nuclear Geochemistry, Sugawara Festival Volume, Maruzen Co., Tokyo.

Jahne, B., Heinz, G., Dietrich, W., 1987. Measurement of the diffusion coefficients of sparingly soluble gases in water. J. Geophys. Res. 92 (C10), 10767–10776.

Keller, C.K., Bacon, D.H., 1998. Soil respiration and georespiration distinguished by transport analyses of vadose CO_2, $^{13}CO_2$, and $^{14}CO_2$. Glob. Biogeochem. Cycles 12 (2), 361–372.

Knapton, A. 2009. Ti Tree Basin Water Resources Report. Department of Natural Resources, Environment, The Arts and Sports, Document number 04/2009A, Northern Territory Government, Australia.

Leaney, F.W., Allison, G.B., 1986. Carbon-14 and stable isotope data for an area in the Murray Basin: its use in estimating recharge. J. Hydrol. 88, 129–145.

Love, A.J., Herczeg, A.L., Armstrong, D., Stadter, F., Mazor, E., 1993. Groundwater flow regime within the Gambier Embayment of the Otway Basin, Australia: evidence from hydraulics and hydrochemistry. J. Hydrol. 143, 297–338.

Mazor, E., 2004. Chemical and Isotopic Groundwater Hydrology, third ed. Marcel Dekker, New York.

Meredith, K., Cendon, D.I., Pigois, J.P., Hollins, S., Jacobsen, G., 2012. Using ^{14}C and ^3H to delineate a recharge 'window' into the Perth Basin aquifers, North Gnangara groundwater system, Western Australia. Sci. Total Environ. 414, 456–469.

Meredith, K., Hollins, S., Cendón, D., 2013. Radiocarbon dating and the challenges in revealing the "age" of groundwater – an example from an evaporation-dominated system in arid Australia., Abstracts Book of the IAEA/RCA Technical Meeting on Processing, Analysis, and Interpretation of Isotopic and Hydrogeochemical Data for Groundwater Dynamics: 4–8 November 2013; Beijing, China, pp. 1–8.

Millington, R.J., Quirk, J.M., 1961. Permeability of porous solids. Trans. Faraday Soc. 57, 1200–1207.

Montfort, J.P., Pellegatta, J.L., 1991. Diffusion coefficients of the halocarbons CCL_2F_2 and C_2Cl_2F4 with simple gases. J. Chem. Eng. Data 36, 135–137.

O'Grady, A.P., Cook, P.G., Eamus, D., Duguid, A., Wischusen, J.D.H., Fass, T., Worldege, D., 2009. Convergence of tree water use within an arid-zone woodland. Oecologica 160, 643–655.

Raich, J.W., Schlesinger, W.H., 1992. The global carbon dioxide flux in soil respiration and its relationship to vegetation and climate. Tellus 44B, 81–99.

Reid, N., Hill, S.M., Lewis, D.M., 2008. Spinifex biogeochemical expressions of buried gold mineralisation: the great mineral exploration penetrator of transported regolith. Appl. Geochem. 23, 76–84.

Scanlon, B.R., Keese, K.E., Flint, A.L., Flint, L.E., Gaye, C.B., Edmunds, W.M., Simmers, I., 2006. Global synthesis of groundwater recharge in semiarid and arid regions. Hydrol. Proc. 20, 3335–3370.

Šimůnek, J., Šejna, M., Saito, H., Sakai, M., Van Genuchten, M. Th., 2013. The HYDRUS-1D Software Package for Simulating the Movement of Water, Heat, and Multiple Solutes in Variably Saturated Media, Version 4.16, HYDRUS

Software Series 3, Department of Environmental Sciences, University of California Riverside, Riverside, California, USA, pp. 340.

Striegl, R.G., Armstrong, D.E., 1990. Carbon dioxide retention and carbon exchange on unsaturated Quaternary sediments. Geochim. Cosmochim. Acta 57, 2277–2283.

Striegl, R.G., Healy, R.W. 1990. Transport of $^{14}CO_2$ in unsaturated glacial and eolian sediments, in chemical modelling of aqueous systems II. In: Melchior, D.C., Bassett, R.L., Am. Chem. Symp. Ser., vol. 416, Am. Chem, Soc., Washington, D.C., pp. 202–210.

Stuiver, M., Pollach, H., 1977. Reporting of ^{14}C data. Radiocarbon 19, 355–363.

Suchomel, K.H., Kreamer, D.K., Long, A., 1990. Production and transport of carbon dioxide in a contaminated vadose zone: a stable and radioactive carbon isotope study. Environ. Sci. Technol. 24, 1824–1831.

Tamers, M.A., 1975. Validity of radiocarbon dates on groundwater. Geophys. Surv. 2, 217–239.

Thorstenson, D.C., Weeks, E.P., Haas, H., Fisher, D.W., 1983. Distribution of gaseous $^{12}CO_2$, $^{13}CO_2$, and $^{14}CO_2$ in the sub-soil unsaturated zone of the Western US Great Plains. Radiocarbon 25 (2), 315–346.

Thorstenson, D.C., Weeks, E.P., Haas, H., Busenber, E., Plummer, L.N., Peters, C.A., 1998. Chemistry of unsaturated zone gases sampled in open boreholes at the crest of Yucca Mountain, Nevada: data and basic concepts of chemical and physical processes in the mountain. Water Resour. Res. 34 (6), 1507–1529.

Trumbore, S., 1993. Comparison of carbon dynamics in tropical and temperate soils using radiocarbon measurements. Glob. Biogeochem. Cycles 7 (2), 275–290.

Van Genuchten, M.Th., 1980. A closed-form equation for predicting the hydraulic conductivity of unsaturated soils. Soil Sci. Soc. Am. J. 44 (5), 892–898.

Vogel, J.C., 1967. Investigations of groundwater flow with radiocarbon. In: Isotopes in Hydrology (Proc. Symp. Vienna, 1966), IAEA, Vienna, pp. 355–369.

Walvoord, M.A., Striegl, R.G., Prudic, D.E., Stonestrom, D.A., 2005. CO_2 dynamics in the Amargosa Desert: fluxes and isotopic speciation in a deep unsaturated zone. Water Resour. Res. 41. http://dx.doi.org/10.1029/2004WR003599.

Warner, M.J., Weiss, R.F., 1985. Solubilities of chlorofluorocarbons 11 and 12 in water and seawater. Deep Sea Res. 32, 1485–1497.

Weeks, E.P., Earp, D.E., Thompson, G.M., 1982. Use of atmospheric fluorocarbons F-11 and F-12 to determines diffusion parameters of the unsaturated zone in the southern high plains of texas. Water Resour. Res. 18 (5), 1365–1378.

Weiss, R.F., 1974. Carbon dioxide in water and seawater: the solubility of a non-ideal gas. Mar. Chem. 2, 203–215.

Yang, W., Amundson, R., Trumbore, S., 1994. A model for soil $^{14}CO_2$ and its implication for using ^{14}C to date pedogenic carbonate. Geochim. Cosmochim. Acta 58, 393–399.

Yang, C, Rattray, G.W., Yu, P., 1996. Interpretation of Chemical and Isotopic Data from Boreholes in the Unsaturated Zone at Yucca Mountain, Nevada. US Geological Survey Water Resources Investigation Report 96–4058, USGS, Denver, Colorado.

Zheng, M., Debruyn, W.J., Saltzman, E.S., 1998. Measurements of the diffusion coefficients of CFC-11 and CFC-12 in pure water and seawater. J. Geophys. Res. 103 (C1), 1375–1379.